Evolutionary Systematics. 7 2023, 237–251 | DOI 10.3897/evolsyst.7.102360

PENSOFT

EVOLUTIONARY SYSTEMATICS

A new species of spiny-backed tree frog, genus *Osteocephalus* (Anura, Hylidae), from the Yanachaga Chemillén National Park in central Peru

Pablo J. Venegas[1,2,3], Luis A. García-Ayachi[2], Eduardo Toral[3], José Malqui[2], Santiago R. Ron[3]

1 *Rainforest Partnership, 4005 Guadalupe St., Austin, Texas 78751, USA*

2 *Instituto Peruano de Herpetología (IPH), Augusto Salazar Bondy 136, Urb. Higuereta, Surco, Lima, Peru*

3 *Museo de Zoología, Escuela de Biología, Facultad de Ciencias Exactas y Naturales, Pontificia Universidad Católica del Ecuador, Av. 12 de Octubre y Roca, Aptdo. 17-01-2184, Quito, Ecuador*

https://zoobank.org/A87192F3-9EFD-4696-B9CE-3A7CA96283B6

Corresponding author: Santiago R. Ron (santiago.r.ron@gmail.com)

Academic editor: Claudia Koch ♦ **Received** 20 February 2023 ♦ **Accepted** 13 June 2023 ♦ **Published** 6 July 2023

Abstract

We describe a new species of *Osteocephalus* Fitzinger, 1843 using morphological traits of adult frogs and its larvae, as well as molecular evidence. The new species occurs in the premontane forest of the Cordillera del Yanachaga in the Andes of central Peru, at elevations between 1000 and 1150 m a.s.l. It belongs to the *Osteocephalus mimeticus* species group and is the sister species of *O. mimeticus*. It is most similar to three species with predominantly dark irises, tuberculate dorsal skin, and brown dorsal coloration: *O. festae* Peracca, 1904, *O. mimeticus* Melin, 1941, and *O. verruciger* Werner, 1901. Of these three species, the most similar is *O. mimeticus*. However, the new species can be easily distinguished from *O. mimeticus* by having a cream or creamy-tan venter with a well-defined pattern of brown chocolate blotches and flecks (venter cream, tan, or brown without marks in *O. mimeticus*). The tadpoles of *O. vasquezi* sp. nov. are strikingly different from the tadpoles of *O. mimeticus* by having a larger oral disk with nine lower labial tooth rows (only six in *O. mimeticus*). Tadpoles of the new species and those of *O. festae* are unique among *Osteocephalus* by belonging to the suctorial ecomorphological guild as shown by their large oral disks. Our time tree suggest that the new species diverged from its sister species at the beginning of the Pleistocene, ~2.5 million years ago.

Key Words

Biodiversity, DNA, new species, *Osteocephalus mimeticus*, phylogeny, tadpole, taxonomy

Introduction

The Neotropical hylid frogs of the genus *Osteocephalus* Fitzinger, 1843 are widely distributed in the Amazon Basin, Guyana region, and Mato Grosso in Brazil (Jungfer et al. 2013). Members of the genus *Osteocephalus* are commonly known as spiny-backed tree frogs, due to the presence of heavily keratinized spicules on the dorsum of breeding males of most species (Jungfer 2010). These nocturnal and arboreal frogs contain 29 nominal species, of which more than half have been resurrected or described since 2000 (Frost 2023). Although most species are restricted to the Amazonian lowlands, some occur in montane forests of up to 2000 m a.s.l. in the eastern Andean slopes (Trueb and Duellman 1971; Jungfer 2010; Ron et al. 2012; Chasiluisa et al. 2020; Frost 2023).

The genus *Osteocephalus* is an important component of the amphibian fauna of the Amazonian and Guyana regions (Jungfer et al. 2013; Ortiz et al. 2022). *Osteocephalus* exhibits a variety of reproductive modes (Jungfer et al. 2013). Some species deposit their eggs in ponds or flooded forest, others in lotic waters. Two clades breed in phytotelmata, including plant axils, bamboo and tree holes and has several forms of parental care (Jungfer and Weygoldt 1999; Jungfer et al. 2000; Moravec et al. 2009; Jungfer et al. 2013; Blotto et al. 2021).

Jungfer et al. (2013) published a phylogeny of *Osteocephalus* and its sister group. They recognized five

Copyright *Pablo J. Venegas et al.* This is an open access article distributed under the terms of the Creative Commons Attribution License (CC BY 4.0), which permits unrestricted use, distribution, and reproduction in any medium, provided the original author and source are credited.

species groups within *Osteocephalus*: *O. alboguttatus*, *O. buckleyi*, *O. leprieurii*, *O. planiceps*, and *O. taurinus*. More recently, Ortiz et al. (2022) removed *O. mimeticus* Melin, 1941, from the *O. buckleyi* group and created the *O. mimeticus* species group. Although it only contains one described and one undescribed species, its time of divergence is similar to that of other species groups in *Osteocephalus*.

Ron et al. (2012), Jungfer et al. (2013), and Ortiz et al. (2022) documented a large number of candidate species within *Osteocephalus*, demonstrating the need for additional systematic studies. Persistent taxonomic problems include undescribed species, binomials of unknown validity, and poorly understood species limits. As a contribution to solving some of those problems, herein, we describe a new species of *Osteocephalus* from Peru using morphological and molecular evidence.

Methods

DNA extraction, amplification, and sequencing

To assess the phylogenetic relationships of the new species, we obtained DNA sequences for nuclear and mitochondrial genes. DNA was extracted from muscle or liver tissue preserved in 95% ethanol or tissue storage buffer using standard phenol-chloroform extraction protocols (Sambrook et al. 1989). We used a polymerase chain reaction (PCR) to amplify DNA fragments for mitochondrial genes 12S RNA, CO1, 16S, ND1, and the nuclear gene POMC. We amplified one DNA fragment for 12S, CO1, and two overlapping fragments for the last ~320 bp of 16S and the adjacent, $tRNA^{Leu}$, ND1, $tRNA^{Ile}$ and $tRNA^{Gln}$ using primers listed in Goebel et al. (1999) and Moen and Wiens (2009). We also amplified the nuclear gene POMC as a single fragment using primers listed by Wiens et al. (2005). For RAG–1 we used primers RS1F (Venkatesh et al. 2001) and WL386 (Moen and Wiens 2009). PCR amplification was carried out under standard protocols. Amplified products were sequenced by the Macrogen Sequencing Team (Macrogen Inc., Seoul, South Korea).

Phylogenetic analyses

Our phylogeny is based on new sequences of *Osteocephalus mimeticus*, *O.* aff. *mimeticus* sensu Ortiz et al. (2022) and the new species described herein. We also included all available GenBank sequences of the *Osteocephalus mimeticus* species group and the mitogenomes of *Osteocephalus* published by Ortiz et al. (2022). We added mitogenomes of *Dryaderces* Jungfer, Faivovich, Padial, Castroviejo-Fisher, Lyra, Berneck, Iglesias, Kok, MacCulloch, Rodrigues, Verdade, Torres-Gastello, Chaparro, Valdujo, Reichle, Moravec, Gvoždík, Gagliardi-Urrutia, Ernst, De la Riva, Means, Lima, Señaris, Wheeler & Haddad, 2013, *Tepuihyla* Ayarzagüena, Señaris & Gorzula, 1993, and *Trachycephalus* Tschudi, 1838, as outgroups (outgroup choice based on Ortiz et al. 2022). The alignment of the sequences was performed in GeneiousPro 9.1.8 (Kearse et al. 2012) with the MAFFT plugin Katoh and Standley (2013). The alignment was manually corrected with Mesquite v.3.02 (Maddison and Maddison 2019) The aligned concatenated final matrix had 38 terminals 14791 bp and is available at Zenodo (http://zenodo.org) under https://doi.org/10.5281/zenodo.7633327. Sample information for GenBank sequences is listed in Ron et al. (2012); Jungfer et al. (2013); and Ortiz et al. (2022). GenBank accession numbers for newly generated sequences are listed in Table 1. Phylogenetic relationships were inferred for all genes concatenated using maximum likelihood (ML) as optimality criterion. We partitioned the matrix by gene or codon position (total number of partitions was 22) and each partition was analyzed under model GTR + G in software IQ-TREE multicore version 2.1.2 (Nguyen et al. 2015; Minh et al. 2020). The ML search was carried out under default settings except for the number of unsuccessful iterations to stop (-nstop 1000) and the perturbation strength (-pers 0.2). We applied the least square dating method (To et al. 2016) to obtain a time tree in IQ-TREE. We used two calibration points based on the phylogeny of Ortiz et al. (2022): 13.1 My for the divergence between *O. taurinus* Steindachner, 1862, and *O.* aff. *cabrerai* and 23.5 My for the divergence between *Trachycephalus* and *Osteocephalus*. To estimate branch support, we made 1000 ultrafast non-parametric bootstrap searches (-*bb* 1000 command;

Table 1. Newly generated DNA sequences of *Osteocephalus vasquezi* sp. nov., *O. mimeticus*, and *O.* aff. *mimeticus* included in phylogenetic analyses. Voucher specimen catalog number and GenBank accession number are shown for each DNA fragment. For collection data see Suppl. material 1.

Voucher number	Species	12S–16S	ND1	CO1	POMC
CORBIDI 6397	*O. mimeticus*	–	OR025569	OR016045	OR025575
CORBIDI 6630	*O.* aff. *mimeticus*	OR018845	OR025566	OR016043	OR025576
CORBIDI 6781	*O. mimeticus*	–	OR025570	OR016046	OR025577
CORBIDI 7095	*O. mimeticus*	–	OR025571	OR016047	OR025578
CORBIDI 7271	*O. vasquezi*	–	OR025572	OR016048	OR025579
CORBIDI 7280	*O. vasquezi*	OR018846	OR025573	OR016049	OR025580
CORBIDI 7284	*O. vasquezi*	OR018847	OR025574	OR016050	OR025581
CORBIDI 8276	*O.* aff. *mimeticus*	–	OR025567	–	OR025582
CORBIDI 8283	*O.* aff. *mimeticus*	–	OR025568	OR016044	OR025583

Hoang et al. 2018) and 1000 replicates for the SH-like approximate likelihood ratio test (*–alrt* 1000 command; Guindon et al. 2010). We considered that branches with bootstrap values > 94 and SH-aLRT values > 79 had strong support. Pairwise uncorrected p-genetic distances for gene 12S RNA were calculated with software MEGA 11.0.13 (Tamura et al. 2021). The standard error of the genetic distance was estimated with the bootstrap method. For accuracy, we only compared overlapping fragments longer than 400 bp. We could not calculate distances for gene 16S because available overlapping fragments were shorter than 400 bp.

Morphological analyses

For ease of comparison of diagnosis and description, we generally follow the format of Trueb and Duellman (1971). Morphological terminology and abbreviations follow Lynch and Duellman (1997) for adults, and Altig and McDiarmid (1999) for tadpoles. Description of oral disk structure follows Altig and McDiarmid (1999). Notation for hand and foot webbing is based on Myers and Duellman (1982). Sex and reproductive condition were determined by the presence of nuptial pads, vocal sac folds, dorsal skin texture, and/or by gonadal inspection. In the species definition, coloration refers to preserved specimens unless otherwise noted. Tadpoles were staged according to Gosner (1960) and preserved in 10% formalin. Adult specimens were fixed in 10% formalin and preserved in 70% ethanol. Morphological data of *Osteocephalus camufatus* Jungfer, Verdade, Faivovich & Rodrigues, 2016, *O. duellmani* Jungfer, 2011, *O. leprieurii* Duméril & Bibron, 1841, *O. melanops* Melo-Sampaio, Ferrão & Moraes, 2021, *O. omega* Duellman, 2019, and *O. vilarsi* Melin, 1941 were taken from literature (Jungfer and Hödl 2002; Jungfer 2011; Jungfer et al. 2016; Duellman 2019; Ferrão et al. 2019; Melo-Sampaio et al. 2021). Examined specimens for comparison are listed in Suppl. material 1 and are housed at the Museo de Zoología, Pontificia Universidad Católica del Ecuador (QCAZ) and the collection of the División de Herpetología, Centro de Ornitología y Biodiversidad (CORBIDI). Morphometric measurements were taken with digital calipers (to the nearest 0.1 mm). We measured the following variables (Duellman 1970): (1) snout-vent length (SVL), (2) head length, (3) head width, (4) tympanum diameter, (5) femur length , (6) tibia length, (7) foot length, (8) eye diameter. Twelve morphometric variables were measured in tadpoles, following Altig and McDiarmid (1999): (1) total length, (2) body length, (3) body width, (4) body height, (5) tail length, (6) eye diameter, (7) oral disc width, (8) interorbital distance, (9) internarial distance, (10) maximum tail height, (11) tail muscle height, (12) tail muscle width.

The tadpole description is based on one lot of tadpoles, deposited at the CORBIDI collection, consisting of 34 larvae in stages (letters in parenthesis refer to individual tadpoles in each lot): 25 (A), 29 (B), 30 (C), 31 (D), 33 (E), 34 (F), 35 (G), 36 (H), 37 (I), 38 (J), 39 (K), 40 (L) and 42 (M). Larval tooth row formula is abbreviated as LTRF throughout. Morphological data of tadpoles of *O. cabrerai* Cochran & Goin, 1970, *O. festae* Peracca, 1904, *O. oophagus* Jungfer & Schiesari, 1995, *O. taurinus*, *O. vilarsi* Melin, 1941 and *O. verruciger* Werner, 1901 were taken from literature (Trueb and Duellman 1970; Henle 1981; Hero 1990; Schiesari et al. 1996; Ron et al. 2010; Ferrão et al. 2019).

Species concept

The taxonomic conclusions of this study are based on the observation of morphological features and phylogenetic relationships. This information is considered as species delimitation criterion following a general lineage or unified species concept (de Queiroz 1998, 2007).

Results

Phylogeny and divergence times

Phylogenetic relationships (Fig. 1) are consistent with Ortiz et al. (2022). We found strong support for the *Osteocephalus mimeticus* species group. *Osteocephalus mimeticus* is sister to the new species, *O. vasquezi* sp. nov. Both species are sister to a seemingly undescribed species, *O.* aff. *mimeticus*, from Cusco department, in southern Peru.

The *O. mimeticus* species group diverged from its sister clade, the *O. buckleyi* species group, ~9.3 My ago. Diversification within the *O. mimeticus* group started ~5 Mya. The new species originated ~2.5 My ago, at the beginning of the Pleistocene. Average uncorrected p-genetic distances for gene 12S, between *O.* aff. *mimeticus* and *O. vasquezi* sp. nov. is 1.67% (SD = 0.39); between *O. vasquezi* sp. nov. and *O. mimeticus* is 2.03% (SD = 0.45). The divergence time between *O. vasquezi* sp. nov. and *O. mimeticus* is at the lower end but within the observed range of divergence between sister species of *Osteocephalus*. That evidence combined with its morphological distinctiveness (see below) indicates that *O. vasquezi* sp. nov. is, in fact, an undescribed species that we describe below.

***Osteocephalus vasquezi* sp. nov.**

https://zoobank.org/BFB20AB6-3458-47FF-BC55-854DE9F75DFE

Figs 2, 4–6A–D

Type material. ***Holotype.*** Peru • Adult male; Pasco department, Oxapampa province, National Park Yanachaga Chemillén, Quebrada Honda (close to the park rangers' checkpoint of Huampal); 9°48'53"S, 75°38'13"W; 1000 m; 15 Aug. 2010; P.J. Venegas, V. Duran, and L. Lujan leg.; CORBIDI 7284 (Fig. 2A, B).

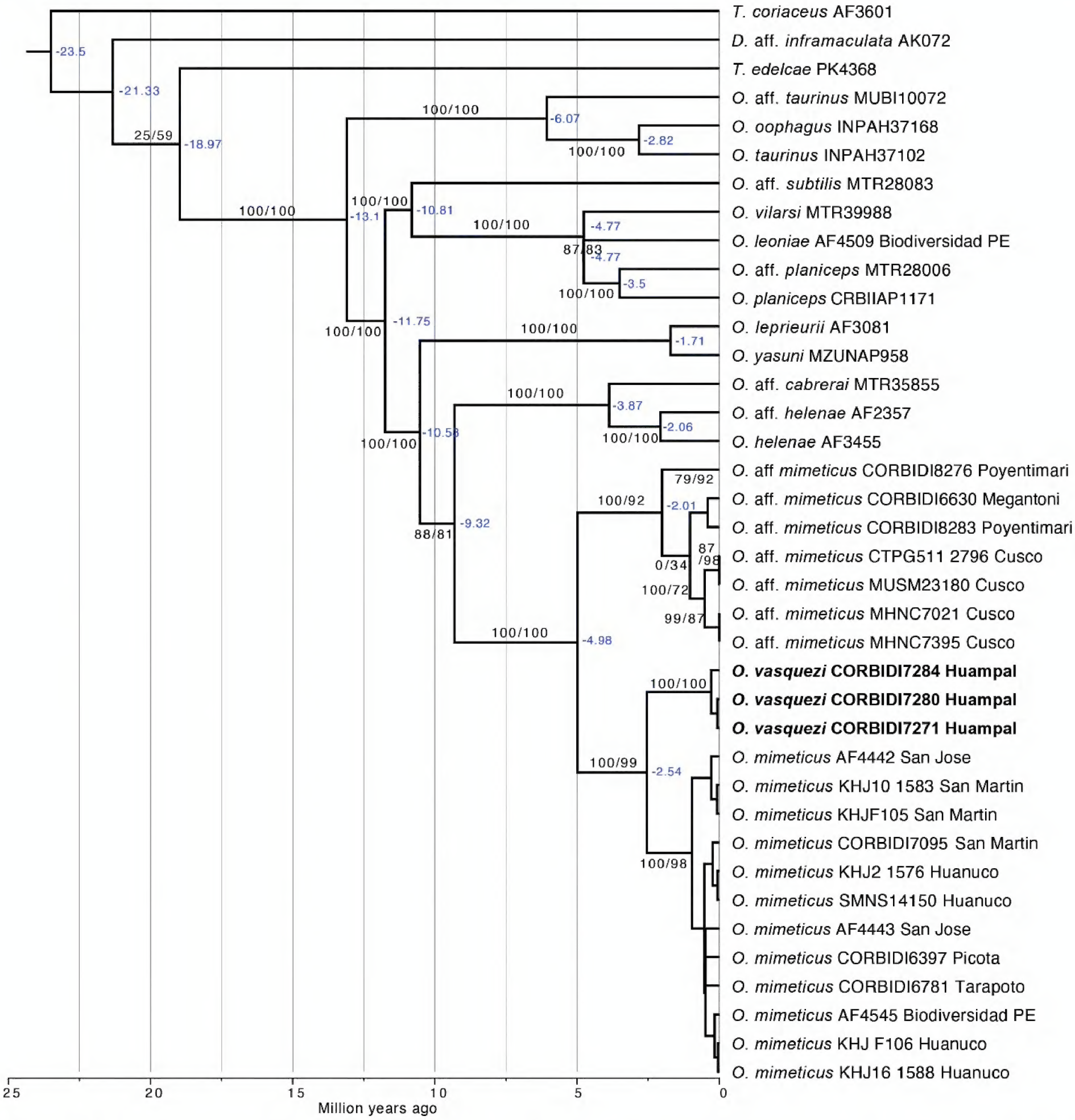

Figure 1. Maximum likelihood Chronogram from analysis of 14791 bp of mitochondrial and nuclear DNA depicting relationships within *Osteocephalus*. Numbers on branches show branch support as percentages: SH-aLRT (before slash) and non-parametric bootstrap support (after). Blue numbers on nodes are estimates of divergence time (in million years). The species name is followed by the number of specimen voucher and the locality.

Paratypes. Peru • 5 ♂♂ adults, 2 ♀♀ adults, 2 juveniles, collected with the holotype; CORBIDI 7270, 7272, 7283, 7285–86, 7271, 7280, 7304, 7438 • 3 ♂ adults, 1 ♀ subadult, collected at the same location of the holotype; 16 Aug. 2010; P.J. Venegas, V. Duran, and L. Lujan leg.; CORBIDI 7277–79, 7275 • 2 ♂♂ adults; Pasco department, Oxapampa province, Quebrada Shuler; 10°10'22"S, 75°34'13"W; 1050 m; 18 Aug. 2010; P.J. Venegas, L. Lujan, and C. Landauro leg.; CORBIDI 7273–74 • 2 ♂♂ adults; Pasco department, Oxapampa province, Quebrada Gallito; 10°13'27"S, 75°35'3"W; 1010 m; 20 Aug. 2010; P.J. Venegas, V. Duran, and C. Landauro leg.; CORBIDI 7276, 7282 • 1 ♂ adult; Pasco department, Oxapampa province, Trocha Colonos; 10°11'03"S, 75°34'27"W; 1050 m; 27 Aug. 2010; P.J. Venegas, V. Duran, L. Lujan, and C. Landauro leg.; CORBIDI 7281.

Definition. *Osteocephalus vasquezi* sp. nov. can be distinguished from its congeners by the following combination of characters: (1) size sexually dimorphic; maximum SVL in males 52.9 mm ($n = 14$), in females 75.5 mm ($n = 2$); (2) skin on dorsum of breeding males bearing conical tubercles with keratinized tips, not present in non-breeding males, smooth in females; (3) skin on flanks weakly areolate in the anterior two-thirds and smooth posteriorly;

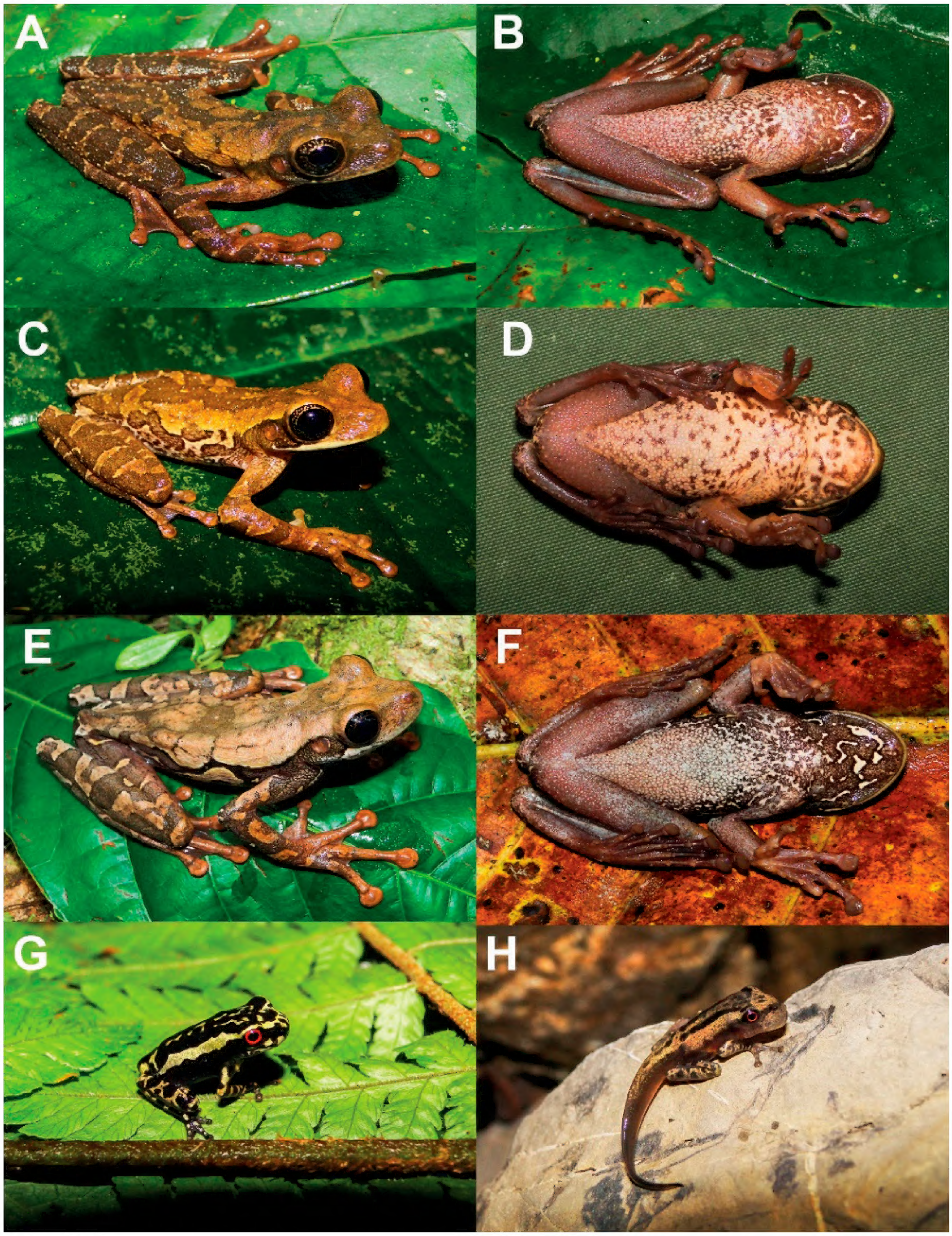

Figure 2. Dorsolateral and ventral views of *Osteocephalus vasquezi* sp. nov. **A, B.** Dorsolateral and ventral view of holotype CORBIDI 7284, SVL = 51.4 mm; **C, D.** Dorsolateral and ventral view of adult male, CORBIDI 7285, SVL = 40.8 mm; **E, F.** Dorsolateral and ventral view of adult female CORBIDI 7280, SVL = 65.9 mm; **G.** Dorsolateral view of a recently metamorphosed CORBIDI 7304, SVL = 13 mm; **H.** Dorsolateral view of tadpole in stage 42. Photographs by P.J. Venegas.

(4) hand webbing formula varies from II2⁻—3⁻III2½—2⁺IV to I basal II2⁻——3⁺III3—2½IV; foot webbing formula varies from I1⁻—1II1⁻—1⁻III0—1⁻IV1⁻—1⁻V to I1—2⁻II1—2⁻III2⁻—2⁻IV2⁻——1V; (5) in life, dorsum varies from brown to dark brown or orange-brown, with or without dark brown irregular marks; (6) throat brown

or tan with a distinctive pattern of white irregular blotches or vermiculations, as well as tan to brown blotches on a whitish cream to creamy tan background; chest and belly cream or creamy tan with chocolate blotches or flecks; (7) cream suborbital mark indistinct, clear labial stripe distinct or faint; (8) color of dorsolateral region of flanks similar to dorsal coloration; ventrolateral region whitish cream or brownish cream with brown scattered blotches and/or vermiculations; (9) dermal roofing bones of the skull not exposed; (10) in life, bones green; (11) in life, iris dark brown with golden vermiculations or flecks; (12) vocal sacs paired, small, located laterally, behind jaw articulation; (13) in life, juveniles with red iris, dorsal surface of body and limbs dark brown (almost black) with marks or coppery with dark brown marks, without conspicuous pale elbows, knees, and heels; (14) larvae with LTRF of 3/9.

Diagnosis. *Osteocephalus vasquezi* sp. nov. is most similar to *O. mimeticus* and *O.* aff. *mimeticus* (see Ortiz et al. 2022). Both species are similar in having dark irises with golden marks (see Fig. 2A–F, 3E–H). However, the new species can be distinguished from *O. mimeticus* in having a cream or creamy-tan venter with a well-defined pattern of brown chocolate blotches and flecks (venter cream, tan, or brown without marks in *O. mimeticus*). Additionally, adult males of *Osteocephalus mimeticus* are larger than those of *O. vasquezi* sp. nov. with non-overlapping ranges [SVL in *O. mimeticus* 58.2–67.5 mm, mean = 63.4 (n = 7), versus 40.9–52.9 mm, mean = 47.9 (n = 13)]. Furthermore, the tadpoles of *O. vasquezi* are strikingly different from the tadpoles of *O. mimeticus* (see Fig. 6) (state of characters between parenthesis) by having: truncate snout in dorsal view (rounded), nostrils oriented dorsolaterally closer to the eyes (nostrils oriented laterally and closer to the end of snout), fins at the posterior third of tail conspicuously narrower (gently narrower), and a higher number of lower labial tooth rows LTRF = 3(3)/9 (LTRF = 2(2)/6).

Other species similar to *Osteocephalus vasquezi* sp. nov. are *O. festae* and *O. verruciger* (Fig. 3), both species of the *Osteocephalus buckleyi* group have predominantly dark irises, tuberculate dorsal skin, and brown dorsal coloration. Although some *O. festae* and *O. verruciger* share with *O. vasquezi* sp. nov. a cream or brownish-cream venter with dark brown chocolate marks, they differ from *O. vasquezi* sp. nov. in having a dark brown iris without bright marks and areolate flanks (iris dark brown with golden vermiculations or flecks, and smooth to weakly areolate in the anterior third of the flank in *O. vasquezi* sp. nov.). Additionally, in *O. festae* and *O. mimeticus* the subocular mark is usually conspicuous, while in the new species it is faint.

Osteocephalus mutabor, *O. omega*, and *O. sangay* Chasiluisa, Caminer, Varela-Jaramillo & Ron, 2020, from the *O. buckleyi* group, also have brown dorsal coloration. However, in life, irises of *O. mutabor* and *O. sangay* are bronze with irregular black reticulations and in *O. omega* are golden yellow, whereas in the new species the irises are dark brown with golden vermiculations or flecks. *Osteocephalus mutabor* also can be readily distinguished by having a dorsal pattern of distinctive transversal stripes (absent in *O. vasquezi* sp. nov.) and lacking dark blotches or flecks on the ventral surface. Additionally, metamorphs and juveniles of *O. mutabor* have green dorsal coloration (black with golden marks in *O. vasquezi* sp. nov.). Females of *O. sangay* have scattered tubercles on dorsum, while females of *O. vasquezi* sp. nov. have the skin of dorsum smooth. Although *O. sangay* also has cream or tan venter with dark brown dots, the new species can be distinguished by its distinctive pattern of white or brown irregular blotches or vermiculations on the throat.

The ventral coloration of *Osteocephalus vasquezi* sp. nov. is shared by some individuals of *O. buckleyi* Boulenger, 1882, *O. cabrerai*, *O. camufatus*, *O. cannatellai* Ron, Venegas, Toral, Read, Ortiz & Manzano, 2012, *Osteocephalus duellmani*, *O. germani* Ron, Venegas, Toral, Read, Ortiz & Manzano, 2012, *O. helenae* Ruthven, 1919, and *O. vilmae* Ron, Venegas, Toral, Read, Ortiz & Manzano, 2012. However, the new species can be easily distinguished, in life, in having a dark brown iris with golden vermiculations or flecks (iris varies from cream to golden or reddish golden and yellow with or without irregular reticulations in the afore listed species, except by *O. duellmani* due to its coloration in life is unknown). Furthermore, *O. buckleyi*, *O. cabrerai*, *O. camufatus*, *O. cannatellai*, *O. helenae*, and *O. vilmae* differ from *O. vasquezi* sp. nov. in having prominent tarsal tubercles (indistinct or absent in the new species). *Osteocephalus cabrerai* also has distinct tubercles on the lower jaw and a fringe in the outer edge of Finger IV, both characters absent in *O. vasquezi* sp. nov. The poorly known *O. duellmani* and *O. germani* have the skin on flanks coarsely areolate or areolate, respectively, and in *O. vasquezi* sp. nov. only weakly areolate in the anterior third of the flank, or completely smooth. Furthermore, *O. duellmani* differs from *O. vasquezi* sp. nov. in having the dorsum shagreen (tuberculate in the new species) and a conspicuous light subocular mark (faint in *O. vasquezi* sp. nov.). In *O. germani* the throat is cream with faint brown flecks, while in the new species is cream with brown blotches or brown with cream vermiculations.

Predominantly dark brown irises are also present in *O. alboguttatus* Boulenger, 1882, *O. heyeri* Lynch, 2002, *O. melanops*, and *O. subtilis* Martins & Cardoso, 1987. *Osteocephalus heyeri* and *O. alboguttatus* can be easily distinguished from the new species by having brown flanks with scattered white blotches (flanks whitish cream or brownish cream with dark brown blotches and vermiculations in *O. vasquezi* sp. nov.). *Osteocephalus subtilis* differs from *O. vasquezi* sp. nov. in having the armpits, groins, anterior and posterior surfaces of thighs, and shanks blue, and the iris dark brown without bright marks. *Osteocephalus melanops* has a cream to white venter, while in the new species it is cream or creamy-tan with brown chocolate blotches and flecks.

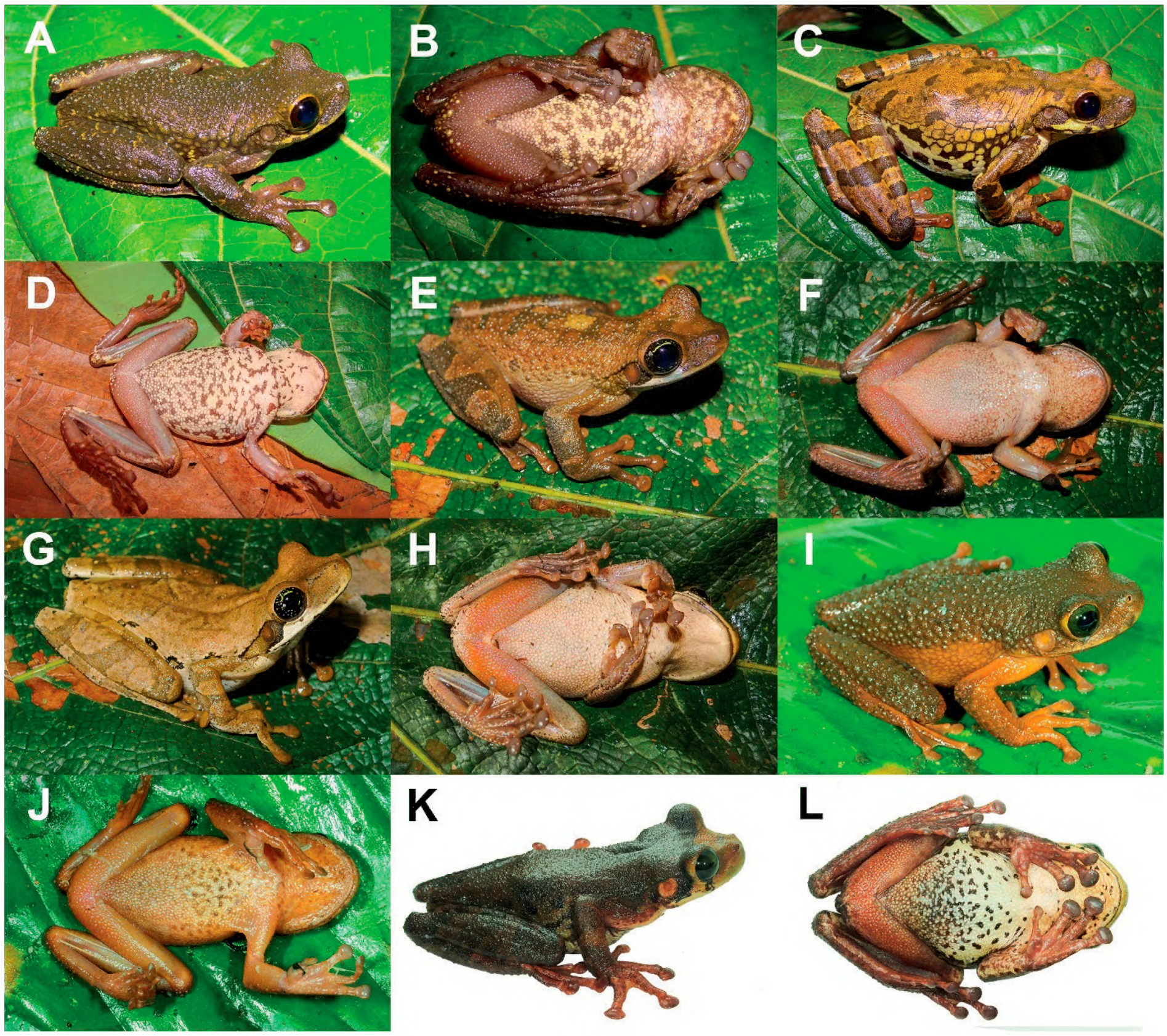

Figure 3. Dorsolateral and ventral views of adult specimens of the four most similar species to *Osteocephalus vasquezi* sp. nov. **A, B.** Male of *O. festae* CORBIDI 758; **C, D.** Female of *O. festae* CORBIDI 761; **E, F.** Male of *O. mimeticus* CORBIDI 9972 from Mishquillaquillo, San Martin; **G, H.** Female of *O. mimeticus* CORBIDI 9970; **I, J.** Male of *O. verruciger* CORBIDI 9477; **K, L.** Female of *O. verruciger* CORBIDI 9525 from Cordillera de Kampankis, Loreto. Photographs **A–H** by P.J. Venegas and **I–L** by A. Catenazzi.

Osteocephalus oophagus, and *O. taurinus* can be easily distinguished from *O. vasquezi* sp. nov. in having bronze to golden irises (clear in preservative) with black lines radiating from the pupil. Furthermore, *Osteocephalus taurinus* differs from *O. vasquezi* sp. nov. in having dermal roofing bones of the skull exposed (not exposed in the new species). *Osteocephalus leprieurii*, and *O. yasuni* Ron & Pramuk, 1999 can be distinguished by their golden to golden brown irises with fine irregular dark venations and a broad dark brown horizontal midline. *Osteocephalus yasuni* also can be distinguished from *O. vasquezi* sp. nov. by its ventral coloration (from yellow to creamy-yellow in *O. yasuni* vs. cream or brownish-cream with chocolate-brown blotches and flecks in *O. vasquezi* sp. nov.) and the color of bones (white in *O. yasuni* and green in *O. vasquezi* sp. nov.). Additionally, *O. leprieurii* and *O. yasuni* breed in ponds and flooded areas (Jungfer et al. 2013), while the new species breeds in torrential streams.

Osteocephalus castaneicola Moravec, Aparicio, Guerrero-Reinhard, Calderón, Jungfer & Gvoždík, 2009, *O. deridens* Jungfer, Ron, Seipp & Almendáriz, 2000, *O. fuscifacies* Jungfer, Ron, Seipp & Almendáriz, 2000, *O. leoniae* Jungfer & Lehr, 2001, *O. planiceps* Cope, 1874, and *O. vilarsi* differ from *O. vasquezi* sp. nov. (characters in parentheses) in having vocal sac single and subgular (vocal sacs paired, located above the arm and below the ear), dorsal skin not sexually dimorphic and more or less smooth in both sexes, except in *O. planiceps* and *O. vilarsi* (dorsal skin sexually dimorphic, strongly tuberculate in males and smooth in females), and breeding in phytotelmata, such as leaf axils, fruit capsules, bamboo and tree holes (Jungfer et al. 2013; Ferrão et al. 2019) (breeding in torrential streams). Additionally, the dark brown iris with golden vermiculation or flecks in *O. vasquezi* sp. nov. differs from the iris of all species in the *O. planiceps* group. Irises are golden to bronze with

fine dark reticulate or black lines radiating from the pupil in *O. castaneicola*, *O. leoniae*, *O. deridens*, *O. fuscifacies*, *O. planiceps*, and *O. vilarsi*.

Of the 29 species of *Osteocephalus* (Frost 2022) known to the date, only the larvae of six species have been formally described (i.e., *O. cabrerai*, *O. festae*, *O. mimeticus*, *O. oophagus*, *O. taurinus* and *O. vilarsi*) (Trueb and Duellman 1970; Henle 1981; Hero 1990; Schiesari et al. 1996; Ron et al. 2010; Ferrão et al. 2019). The tadpoles of *O. vasquezi* sp. nov. differ from its congeners by the following characters: truncate snout in dorsal view (except for *O. oophagus*, in the rest of species it is rounded), nostrils oriented dorsolaterally closer to the eyes than the end of snout (nostrils oriented laterally in the rest of species, closer to the end of snout in *O. cabrerai*, *O. mimeticus*, and *O. vilarsi*, and intermediate in *O. taurinus* and *O. verruciger*), fins at the posterior third of tail conspicuously narrower (except for *O. festae*, in the other species fins are gently narrower). Furthermore, *O. vasquezi* sp. nov. has a higher number of lower labial tooth rows: LTRF = 3(3)/9 vs. LTRF = 2(2)/6(1) in *O. cabrerai*, 4–5/7 in *O. festae*, 2(2)/6 in *O. mimeticus*, 2(2)/6 in *O. oophagus* and 2(2)/3–7(1) in *O. taurinus*, 2(2)/5–6(1) in *O. vilarsi*, and 2(2)/5(1) in *O. verruciger*.

Description of holotype. Adult male (Figs 4, 5), 51.4 mm SVL, head length 15.5 mm, head width 15.5 mm, eye diameter 5.3 mm, tympanum diameter 3.1 mm, femur length 23.7 mm, tibia length 28.0 mm, foot length 22.3 mm. Head narrower than body; snout truncate in lateral and dorsal views; canthus rostralis distinct and rounded; loreal region concave; internarial area depressed; nostrils slightly protuberant, directed laterally; interorbital area flat, with scattered small tubercles, lateral margins of the frontoparietals inconspicuous through skin; eye strongly protuberant; tympanic membrane evident, slightly wider than high, separated from eye by ca. 93% of its diameter; tympanic annulus distinct. Tongue cordiform, widely attached to floor of mouth; vomerine odontophores angular, adjacent medially, posteromedial to choanae, bearing 9 and 8 (left/right) vomerine teeth; choanae with capsular shape, oblique; deflated vocal sacs distinct above the arms and below the ears.

Axillary membrane present, reaching half the arm length; ulnar tubercles absent; relative length of fingers I < II < IV < III (Fig. 4); fingers bearing oval discs, that of Finger III about two thirds of tympanum diameter; subarticular tubercles prominent, round to ovoid except for slightly bifid distal subarticular tubercle of Finger IV; supernumerary tubercles present, distinct; palmar tubercle elongated; prepollical tubercle protuberant, elliptical; prepollex present; dark brown, keratinous nuptial excrescences covering inner surface of prepollex up to the intercalary cartilage of thumb; webbing basal between fingers I and II; webbing formula of fingers **II**2^{-}—3**III**3^{-}—**2½IV** (Fig. 4).

Small tubercles on tibiotarsal articulation; dorsal surface of tarsus covered by scattered minute keratinized conical tubercles, more abundant on outer edge; small tubercles scattered along ventrolateral edge of foot; toes bearing discs slightly wider than long, smaller than those of fingers; relative length of toes I < II < V < III < IV; outer metatarsal tubercle ill defined, small, round; inner metatarsal tubercle larger, ovoid; subarticular tubercles single, round, protuberant; supernumerary tubercles restricted to the soles; webbing formula of toes **I**1—1^{+}**II**1—1^{+}**III**1—1^{+}**IV**1^{+}—1**V** (Fig. 4).

Skin on dorsum, head, and dorsal surfaces of hindlimbs shagreen, covered by conical tubercles with keratinized tips, tubercles minute on head and limbs; skin on flanks weakly areolate; skin on venter granular; skin on ventral

Figure 4. Ventral views of right hand and foot of *Osteocephalus vasquezi* sp. nov. holotype (CORBIDI 7284). Scale bar: 10 mm.

surfaces of head smooth, on those of thighs smooth on the anterior half and granular on the posterior half, smooth on shanks. Cloacal opening directed posteriorly at upper level of thighs; short simple cloacal sheath covering cloacal opening; round tubercles around vent and on posterior surface of proximal third of thighs.

Color of holotype in life. Based on digital photographs (Fig. 2A, B). Dorsal surface of head dark brown, dorsum brown with dark brown irregular blotches, dorsal surfaces of limbs brown with dark brown diagonal bars; sides of head dark brown with pale lips and a thin white subocular stripe, upper flanks brown, mid- and lower-flanks dark brown with scattered vermicular white blotches. Venter light cream with chocolate blotches and flecks, more abundant on chest; throat dark brown with white vermiculations; ventral surface of limbs, palms, and soles brown. Iris dark brown with irregular golden vermiculation.

Color of holotype in preservative. Dorsal surface of head dark brown, dorsum pale brown with dark brown irregular marks, dorsal surface of limbs pale brown with dark brown diagonal bars; sides of head dark brown with pale lips and a thin white subocular stripe, flanks dark brown with scattered vermicular white blotches. Venter dirty cream with chocolate blotches and flecks more abundant on the chest; throat brown with white vermiculations; ventral surface of limbs brownish cream, palms and soles brown.

Variation. Variation in dorsal and ventral coloration of preserved specimens is shown in Fig. 5. Dorsal background coloration varies from grayish-brown to brown or dark brown, irregular dark brown marks usually present. One specimen (CORBIDI 7276) has brownish-cream scattered blotches on dorsum; CORBIDI 7273 and 7278 have pale brown dorsum without dark marks; CORBIDI 7271 with scattered faint vermiculations on dorsum. Ventral surfaces of preserved specimens (Fig. 5) vary from light cream to dirty cream with scattered chocolate-colored blotches, spots, or flecks; one specimen (CORBIDI 7274) has a cream venter with faint blotches. Some specimens (e.g., CORBIDI 7275, 7277) have venters densely spotted, the two adult females (CORBIDI 7271, 7280) have finely reticulated venters. Throat coloration light cream with faint chocolate blotches on sides of throat (CORBIDI 7271, 7282), or light cream with scattered chocolate blotches (CORBIDI 7277, 7278, 7283, 7286), or dark brown (CORBIDI 7280, 7281) or pale brown with white vermiculations (CORBIDI 7276). Undersides of limbs vary from cream to brownish-cream. Cream-colored low tubercles on the outside edge of the forearm present only in CORBIDI 7275. The skin of the anterior and posterior surfaces of thighs and concealed surfaces of shanks is light cream or brownish-cream. The vent region is usually dark brown surrounded by a light cream edge; CORBIDI 7283 has the vent region dirty cream. Background color of flanks varies from grayish-cream to brownish-cream; some specimens (CORBIDI 7273, 7282, 7280, 7271) have a long undulating longitudinal dark brown stripe along the flanks; CORBIDI 7274 has scattered circular blotches along the flanks; the rest of the specimens have irregular dark brown or pale brown blotches along the flanks. Lateral head coloration varies from brown to dark brown. The subocular white mark varies from a thin stripe (e.g., CORBIDI 7276) to a faint blotch (e.g., CORBIDI 7272), and some specimens have little brown spots on the subocular blotch (e.g., CORBIDI 7277, 7281).

The only known adult females ($n = 2$) lack tubercles on dorsum, while in males the dorsum varies between lacking tubercles (CORBIDI 7275, 7279) to having well defined tubercles with a keratinized spicule on the tip (e.g., CORBIDI 7283). The skin on the flanks is weakly areolate to areolate in the anterior one-third and smooth posteriorly. The two adult females (CORBIDI 7272, 7280) have smooth flanks. Head shape is truncate in dorsal and lateral view as in the holotype. The tympanic annulus is concealed dorsally by a supratympanic fold and is of a lighter color than the background. The distal subarticular tubercle on Finger IV is slightly bifid in all specimens. Measurements and proportions of the type series of *Osteocephalus vasquezi* sp. nov. are summarized in Table 2. In the examined series, the largest male has a SVL of 52.9 mm and the largest female 75.5 mm; mean adult male SVL = 48.1 mm ($n = 14$, SD = 3.86), mean adult female SVL = 70.7 mm ($n = 2$).

Based on digital photographs of the adult specimens in life (Fig. 2A–F), the dorsal background color of body and limbs varies from pale brown (CORBIDI 7273) to dark brown (CORBIDI 7272) or orange-brown (CORBIDI 7270), with or without dark brown irregular marks on dorsum and dark brown or faint brown transversal bands on limbs; dorsal surface of head is darker than body in some specimens (e.g., CORBIDI 7271), sides of head are darker than body in some specimens, especially in the tympanic region; flanks are pale brown in all specimens with the upper region brownish-cream or whitish-cream with scattered dark brown irregular blotches (ill-defined in CORBIDI 7273); throat usually whitish cream with brown or dark brown irregular blotches, some specimens (e.g., CORBIDI 7280) have the throat brown with irregular white blotches; chest and belly vary from cream to whitish-cream or dirty cream with scattered brown blotches, spots, and flecks or with fine brown reticulations on the belly (e.g., CORBIDI 7272, 7271). The nuptial pad is cream or brownish cream and contrasts with the background brown color of the thumb and rest of the fingers. Iris dark brown with golden vermiculations or flecks.

There is significant change in color between juveniles and adults. The following description is based on a digital photograph of juvenile CORBIDI 7304 (Fig. 2G). Top of head, body, and limbs dark brown (almost black) with golden marks as dorsolateral irregular stripes, from the tip of snout to the posterior end of the sacrum, scattered vermiculations, transverse bands on limbs, and golden labial marks; venter dark brown, almost black; iris bright red.

Figure 5. Preserved specimens of *Osteocephalus vasquezi* sp. nov. showing variation in dorsal and ventral pattern. Left to right, first row: CORBIDI 7271 (female), 7280 (female), 7274, 7276, and the holotype 7284 (males); second row CORBIDI 7277, 7278, 7279, 7281, 7283 (males); third row: CORBIDI 7271 (female), 7280 (female), 7274, 7276, and the holotype 7284 (males); fourth row: CORBIDI 7277, 7278, 7279, 7281, 7283 (males). All specimens are shown at the same scale.

Tadpoles. Tadpoles were collected at Quebrada Honda, the same location as for the holotype, on 20 August 2010. These larvae belong to the exotrophic, lotic, suctorial guild as defined by Altig and McDiarmid (1999). Guild assignment was based on oral disk and body morphology. Morphometric data are provided in Table 3.

In dorsal view, a tadpole in Stage 33 (Fig. 6A–D) shows an elliptical body, widest between eye and spiracle, with a rounded snout. Eyes are relatively large (BL about 10.4 times larger than ED), separated by a distance 1.34 times the internarial distance, directed and positioned dorsolaterally, not visible in ventral view. External nares oval, located dorsolaterally, at about one fourth the distance between anterior margin of snout and anterior margin of eye.

In profile (Fig. 6B) body depressed (BW/BH = 1.35), flattened ventrally, snout slightly rounded. Oral disc not emarginated. Spiracle single, sinistral, inner wall free

Table 2. Measurements of adult *Osteocephalus vasquezi* sp. nov. and *O. mimeticus*. Averages are followed by standard deviation and ranges. Abbreviations are: SVL = Snout-vent length; HL = Head length; HW = Head width; ED = Eye diameter; TD = Tympanum diameter; TL = Tibia length; FL = Femur length; FOOT = Foot length. All measurements are in mm.

	O. vasquezi sp. nov.		*O. mimeticus*		*O.* aff. *mimeticus*	
	male (n = 13)	female (n = 2)	male (n = 7)	female (n = 5)	male (n = 9)	female (n = 1)
SVL	47.9 ± 3.9; 40.9–52.9	70.8 ± 6.8; 66.0–75.6	63.4 ± 3; 58.2–67.5	72.1 ± 7.01; 61.6–78.6	60.1 ± 6.5; 52.4–75.1	67.6
HL	15.0 ± 1.1; 12.9–16.1	21.4 ± 2.3; 19.8–23.1	20.2 ± 1.1; 18.4–21.9	31.3 ± 1.9; 19.5–24.5	19.2 ± 1.5; 17.3–22.0	21.0
HW	14.8 ± 1.1; 12.6–16.1	21.9 ± 2.3; 20.2–23.5	20.7 ± 1; 19.2–22.0	22.7 ± 2.1; 20.4–25.7	19.2 ± 1.8; 17.2–23.0	20.6
ED	5.1 ± 0.5; 4.5–6.1	6.6 ± 0.7; 6.1–7.1	6.2 ± 0.5; 5.6–6.9	23.5 ± 2.4; 5.6–11.4	6.1 ± 0.6; 5.1–6.7	5.5
TD	2.8 ± 0.2; 2.3–3.2	3.7 ± 0.2; 3.6–3.9	4.5 ± 0.4; 3.7–4.9	7.3 ± 2.4; 4.2–10.1	4.2 ± 0.4; 3.6–4.6	3.7
TL	26.1 ± 2.5; 22.2–29.3	40.4 ± 3.6; 37.9–42.9	34.7 ± 2.1; 32.0–37.3	5.8 ± 5.7; 35.5–50.1	32.5 ± 3.5; 29.1–39.6	39
FL	22.7 ± 1.9; 19.9–25.7	37.3 ± 1.06; 36.6–38.1	27.0 ± 1.7; 24.9–30.0	42.9 ± 6.6; 30.1–47.3	31.0 ± 3.2; 27.7–38.3	36.6
FOOT	20.9 ± 1.9; 17.4–23.1	31.3 ± 3.5; 28.8–33.8	26.2 ± 1.2; 24.5–28.3	72.1 ± 3.2; 26.5–34.5	25.6 ± 2.4; 23.5–31.5	29.6
HL/SVL	0.3 ± 0.3; 0.30–0.33	0.3 ± 0.3; 0.30–0.31	0.3 ± 0.4; 0.31–0.32	0.4 ± 0.3; 0.31–0.32	0.32 ± 0.01; 0.29–0.34	0.31
HW/SVL	0.3 ± 0.3; 0.30–0.32	0.3 ± 0.3; 0.3–0.3	0.3 ± 0.3; 0.32–0.33	0.3 ± 0.3; 0.32–0.33	0.32 ± 0.01; 0.31–0.34	0.30
TD/ED	0.6 ± 0.5; 0.5–0.6	0.2 ± 0.3; 0.5–0.6	0.7 ± 0.8; 0.6–0.8	39.2 ± 1; 0.4–1.6	0.69 ± 0.05; 0.61–0.78	0.68
TL/SVL	0.5 ± 0.6; 0.5–0.6	0.1 ± 0.5; 0.6–0.6	0.5 ± 0.7; 0.5–0.6	0.3 ± 0.8; 0.6–0.7	0.54 ± 0.02; 0.52–0.58	0.58
FL/SVL	0.5 ± 0.5; 0.4–0.5	0.5 ± 0.2; 0.5–0.6	0.4 ± 0.6; 0.4–0.5	0.9 ± 0.9; 0.5–0.6	0.52 ± 0.01; 0.50–0.53	0.54
FOOT/SVL	0.4 ± 0.5; 0.4–0.5	0.5 ± 0.5; 0.4–0.4	0.4 ± 0.4; 0–39–0.43	0.6 ± 0.5; 0.43–0.44	0.43 ± 0.01; 0.42–0.45	0.44

Table 3. Measurements (in mm) of developmental stages between parentheses (sensu Gosner, 1960) of 13 tadpoles (lot CORBIDI 24671) of *Osteocephalus vasquezi* sp. nov. Abbreviations are: TL = total length; BL = body length; BW = Body width; BH = body height; TAL = tail length; ED = eye diameter; ODW = oral disc width; IOD = interorbital distance (measured between center pupils); IND = internarial distance (measured between centers of narial apertures); MTH = maximum tail height; TMH = tail muscle height; TMW = tail muscle width.

	Stage												
Variable	**A (25)**	**B (29)**	**C (30)**	**D (31)**	**E (33)**	**F (34)**	**G (35)**	**H (36)**	**I (37)**	**J (38)**	**K (39)**	**L (40)**	**M (42)**
TL	23.8	28.4	29.6	32.4	36.1	34.4	35.4	37.9	38.7	36.8	39.6	39.7	41.1
BL	8.3	10.7	10.7	11.6	12.4	12.8	12.7	13.2	13.9	13.8	14.1	13.9	14.5
BW	5.2	6.5	6.7	6.7	7.5	7.5	7.7	7.9	7.8	8.5	8.4	8.3	7.8
BH	3.4	4.8	4.8	5.3	5.5	6.3	6.2	6.3	6.6	6.0	6.4	6.1	6.3
TAL	15.4	17.6	19.0	20.8	23.7	21.6	22.7	24.7	24.8	23.0	25.6	26.4	26.6
ED	0.7	1.2	1.0	1.1	1.2	1.5	1.6	1.6	1.7	1.8	1.8	1.8	2.2
ODW	5.2	5.9	6.0	6.4	6.3	6.9	7.0	7.2	7.6	7.8	7.3	6.6	6.0
IOD	3.6	4.3	4.4	4.8	5.2	5.4	5.4	5.4	5.6	5.1	5.6	5.6	6.3
IND	2.8	3.4	3.4	3.6	3.9	4.0	3.8	3.9	4.0	4.0	4.1	3.6	1.8
MTH	3.7	4.8	4.8	5.3	5.8	6.0	6.2	5.8	6.4	6.0	6.4	7.0	6.3
TMH	2.2	3.0	2.9	3.0	3.3	3.4	3.4	3.6	3.8	3.7	3.7	3.7	3.7
TMW	1.8	2.4	2.5	2.8	2.8	3.3	3.1	3.2	3.5	3.3	3.5	3.5	4.2

from body, its tip closer to the vent than the eye. Spiracle opening rounded, at level of the forelimbs. Tail musculature robust up to first one third, decreasing in size towards the tip of tail. Dorsal fin does not extend onto the body, slightly convex, and reaches its highest width up the half of tail. Tail tip acuminate. Ventral fin slightly convex, beginning in the tail-body junction and tapering abruptly in the last third towards the tail tip. Vent tube medial, with both walls attached directly to ventral fin, opening directed posteroventrally. Lateral line system present on: dorsal body, middle body; supraorbital, infraorbital, posterior supraorbital; and posterior infraorbital. No glands.

Oral disc anteroventral (Fig. 6C, D); transverse width 5.6 mm; 70.86% of BW), not emarginated, LTRF 3(3)/9; papillae distributed around oral disc; tooth rows complete except for medial gap in row A3; A1 = 778, A2 = 592, A3 = 195 + 203; P1 = 267, P2 = 325, P3 = 336, P4 = 380, P5 = 323, P6 = 409, P7 = 316, P8 = 493 and P9 = 296.

Based on PJV's field notes of tadpoles the color in life between stages 30 to 42 (Fig. 2H, Stage 42): dorsal surface of head, body, limbs, and base of tail light coppery with black marks, flanks and sides of tail brown, venter brown and slightly translucent, iris red. Tadpoles in stages 31, 35, and 37 have a dark brown dorsum, venter brown with the gut visible; tail musculature brown, lighter than the dorsum; fins translucent with a pale brown tone. Tadpoles in stages 39 and 40 have the same coloration as of the aforementioned stages but with a pale dorsolateral stripe on each side.

Dorsum pale brown, caudal muscle beige with brown spots (Fig. 6A–C). Eyes, flanks, spiracle, vent tube, fins, and venter dark brown surrounded by transparent areas. Venter and fin transparent.

Distribution and natural history. *Osteocephalus vasquezi* sp. nov. is only known from the type locality in Cordillera de Yanachaga, Pasco department, at elevations between 1000 and 1150 m, in the upper Amazon basin of central Peru (Fig. 7). This new species inhabits the premontane forest of the Río Huancabamba canyon. The distribution lies within the Yanachaga Chemi-

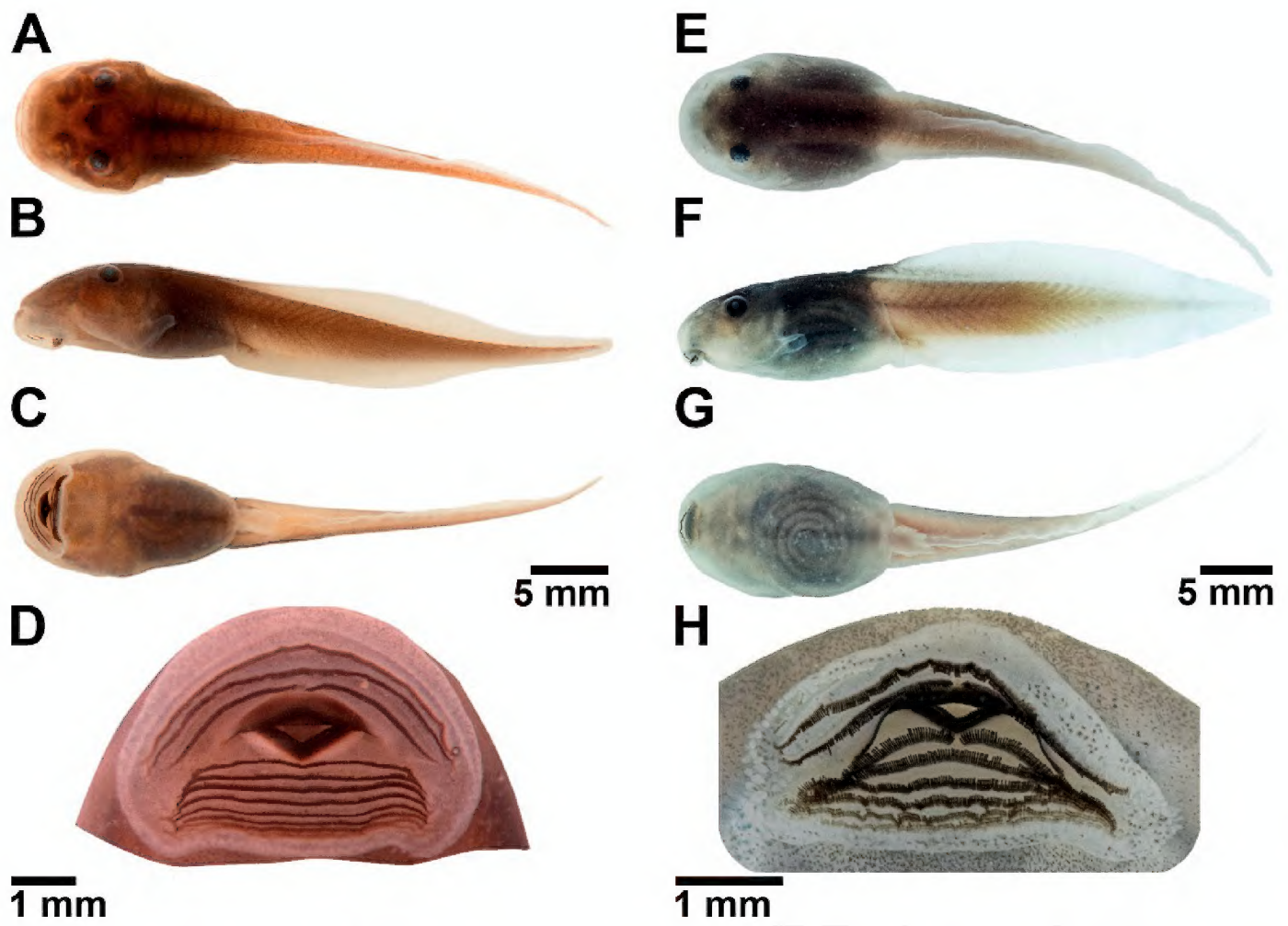

Figure 6. Preserved tadpoles of *Osteocephalus vasquezi* sp. nov. and *O. mimeticus*. **A–D.** *Osteocephalus vasquezi* stage 33, CORBIDI 24671; **E–H.** *O. mimeticus*, stage 33, CORBIDI 24672. **A, E.** Dorsal view; **B, F.** Lateral view; **C, G**. Ventral view; **D, H.** Oral apparatus. Photographs of *O. vasquezi* by E. Toral and *O. mimeticus* of L. García-Ayachi.

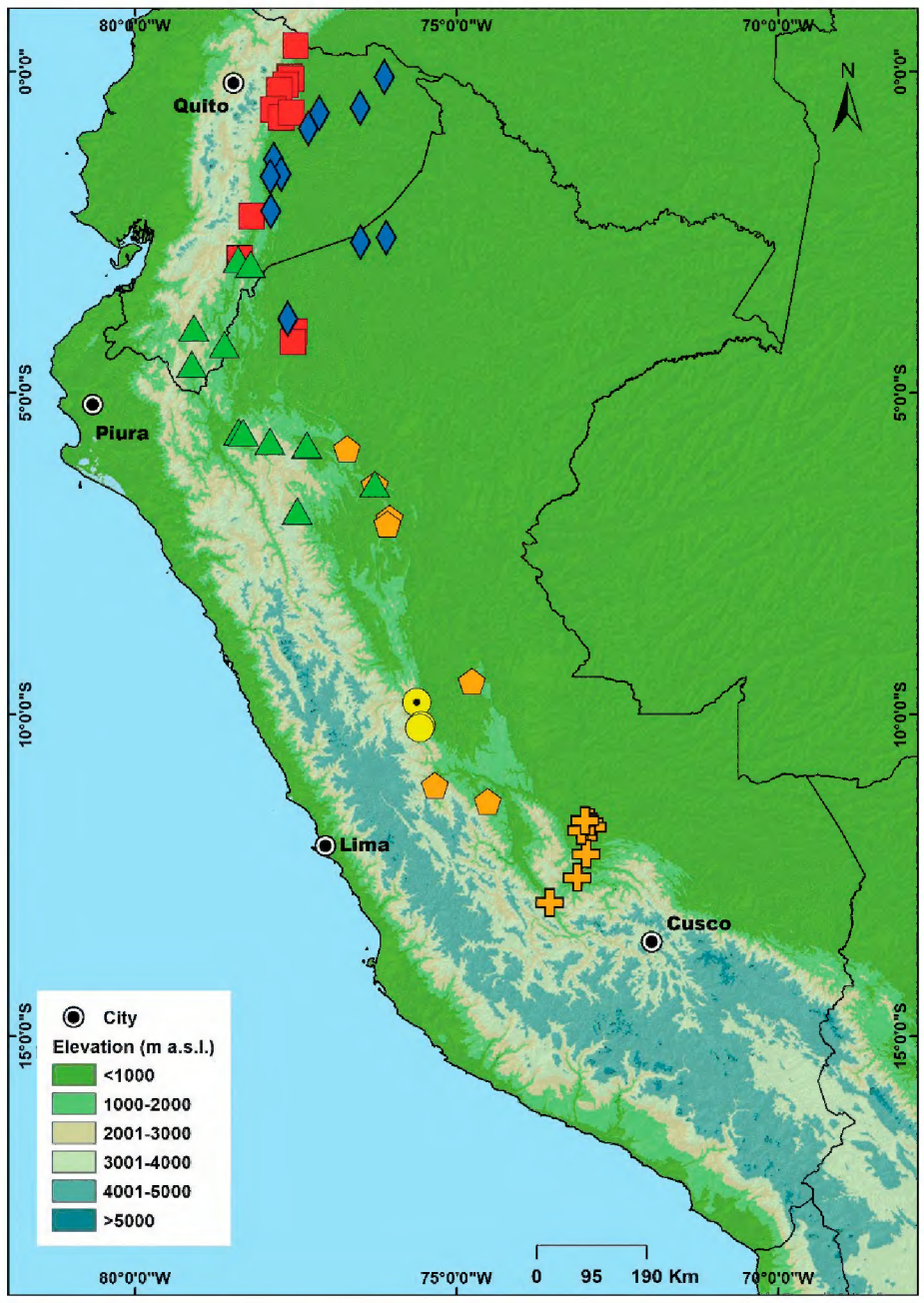

Figure 7. Records of *Osteocephalus vasquezi* sp. nov. (circles; type locality with a dot), *O. festae* (triangles), *O. mimeticus* (pentagons), *O.* aff. *mimeticus* (crosses), *O. mutabor* (diamonds) and *O. verruciger* (squares). Locality data from specimens deposited at the Centro de Ornitologia y Biodiversidad and Museo de Zoología of Pontificia Universidad Católica del Ecuador. (Suppl. material 1).

llén National Park and in the ecoregions of Selva Alta (400–1000 m) and Yungas (500–2300 m), according to Brack-Egg (1986) and Peñaherrera del Aguila (1989). All individuals were collected at night, on leaves and branches of bushes up to 2 m above the ground, along ravines in Quebrada Honda and Quebrada Shuler, both drainages of the Río Huancabamba. Sympatric amphibians were *Bolitoglossa peruviana* Boulenger, 1883, *Leptodactylus rhodonotus* Günther, 1869, *Pristimantis diadematus* Jiménez de la Espada, 1875, *P. minutulus* Duellman & Hedges, 2007, *Pristimantis* sp., *Rhinella* aff. *leptoscelis* Boulenger, 1912, and *R. poeppigii* Tschudi, 1845. Recently metamorphosed juveniles of *Osteocephalus vasquezi* sp. nov. were on the rocks and leaves of low bushes on the shores of Quebrada Honda on the second half of August. The ravine of Quebrada Honda has a torrential stream of clear waters and a rocky bottom. Tadpoles of *O. vasquezi* sp. nov. were observed adhered to rocks, presumably with their oral disk, in the narrow and very torrential portion of Quebrada Honda and in the Huancabamba River. Tadpoles of *Rhinella* aff. *leptoscelis* were found in the same stream, but in lower abundance.

Etymology. The specific name is a patronym for Pedro Vásquez Ruesta, a Peruvian forest engineer, who is a pioneer in the wildlife management in Peru. Since 1978 he has worked for the development of wildlife management and protected natural areas as a professor at the Faculty of Forestry at Universidad Nacional Agraria La Molina, Lima, Peru, teaching to generations of forest engineers about wildlife management and conservation. During his academic life, Pedro Vásquez Ruesta made many contributions to the field of conservation of natural resources,

advising theses and published scientific articles especially about the management of caimans and deer.

Discussion

Although the alpha taxonomy and systematics of *Osteocephalus* has advanced considerably in the last two decades (e.g., Jungfer 2011; Ron et al. 2012; Jungfer et al. 2013; Blotto et al. 2021; Ortiz et al. 2022), cryptic diversity and taxonomic problems (e.g., undescribed species, validity of poorly know binomials, and unclear species limits) remain as an obstacle to understand the real diversity of this genus. Recent systematics publication reveal a large number of candidate species (Ron et al. 2012; Jungfer et al. 2013; Blotto et al. 2021; Ortiz et al. 2022) and well identified species complexes (e.g., *O. verruciger-cannatellai* complex and *O. helenae* complex) (Chasiluisa et al. 2020; Ortiz et al. 2022).

Jungfer et al. (2013); and Ortiz et al. (2022) show two well supported clades, a northern and a southern clade, for *O. mimeticus*. In our maximum likelihood phylogeny (Fig. 1), *O. mimeticus* is paraphyletic relative to *O. vasquezi* sp. nov. showing the northern clade, conformed by specimens of San Martín and Huánuco (*O. mimeticus sensu stricto*), as sister of *O.* aff. *mimeticus* clade that contains specimens from Cusco of southern Peru. Average genetic distance (12S) between the clade of *O. mimeticus sensu stricto* and *O. vasquezi* sp. nov. is 2.03%. The genetic distance between both species is at the lower end of the range of distances between sister species of *Osteocephalus*. We corroborate the separation of *O. vasquezi* sp. nov. as a different species with unequivocal morphological evidence: ventral pattern of adult individuals and larval anatomy, both taxonomic characters widely used for diagnosed species in hylid frogs (Ron et al. 2010; Lehr et al. 2011; Coloma et al. 2012; Caminer and Ron 2014).

The phylogenetic position of *O. vasquezi* sp. nov. is consistent with Ortiz et al. (2022) in showing that populations from Cusco, similar to *O. mimeticus*, likely represent a new species (*O.* aff. *mimeticus* in Fig. 1). In our comparisons of *O. mimeticus*, we noted that the venter of *O.* aff. *mimeticus* is a bit darker than that of *O. mimeticus* (bright cream to cream with faint brown flecks in *O. mimeticus* vs. tan or chocolate venter in *O.* aff. *mimeticus*). However, the description of *O.* aff. *mimeticus* would need additional lines of evidence (e.g., improved phylogenetic sampling, comparative tadpole morphology and, if possible, advertisement calls).

The genus *Osteocephalus* uses different kinds of water bodies for reproduction and exhibits a variety of reproductive modes that are phylogenetically conserved (Ron et al. 2010; 2012; Jungfer et al. 2013). In fact, most species deposit their eggs in lentic or lotic waters (Henle 1981; Jungfer 2010; Ron et al. 2010; Menin et al. 2011) and some in phytotelmata (Jungfer and Weygoldt 1999; Jungfer et al. 2000; Moravec et al. 2009). Stream and pond-dwelling tadpoles of *Osteocephalus* are generalist omnivorous and share similar numbers of tooth rows (Trueb and Duellman 1970; Henle 1981; Hero 1990; Ron et al. 2010; Menin et al. 2011), whereas phytotelma adapted tadpoles are highly specialized exotrophic feeders of subsequent egg depositions of the conspecific parent and possess a reduced number of labial tooth rows (Jungfer and Schiesari 1995; Schiesari et al. 1996). Although currently, only 20% of the *Osteocephalus* tadpoles have been described, they exhibit conspicuous adaptations to their diet and habitat (Ron et al. 2010; Jungfer et al. 2013). In the *O. buckleyi* and the *O. mimeticus* species group, most of the species with reproduction data available are associated with streams (Trueb and Duellman 1970; Henle 1981; Jungfer 2010; Ron et al. 2010; Menin et al. 2011; Lima et al. 2012). Their tadpoles show ecomorphological adaptations to the lotic habitats where they live. For example, tadpoles of *O. cabrerai*, *O. mimeticus*, *O. mutabor*, and *O. verruciger* live in shallow waters of medium to slow currents (e.g., inlets along the stream banks or slow flowing ditches) and even in ponds on stream banks (Trueb and Duellman 1970; Henle 1981; Ron et al. 2010; Menin et al. 2011; Villacampa Ortega et al. 2013; Venegas pers. obs.). The aforementioned species belong to the ecomorphological guild of adherent tadpoles (*sensu* Altig and Johnston 1989) that has a smaller oral disc and live in flowing water of medium to slow currents or even in ponds alongside streams. In contrast, the tadpoles of *O. festae* and *O. vasquezi* sp. nov. live in fast water of rocky streams and belong to the suctorial ecomorphological guild, as defined by Altig and Johnston (1989), that include the lotic rheophilous tadpoles. Both species are endowed with large oral discs (58% and 70.86% of body width in *O. festae* and *O. vasquezi* sp. nov., respectively) and depressed bodies that permit adhering to rocks and feed in strong currents (Altig and McDiarmid 1999). Furthermore, the suctorial tadpoles of *O. festae* and *O. vasquezi* sp. nov. also exhibit more labial tooths rows (LTRF = 3(3)/9 in *O. vasquezi* sp. nov. and 4–5/7 in *O. festae*), strong caudal musculature (see Fig. 6A), and conspicuously narrower fins on the posterior third of tail (see figs 6B and 5F in Ron et al. 2010). Therefore, the tadpoles of both species seem to represent the most specialized *Osteocephalus* tadpole form know to date.

Acknowledgements

Laboratory work in Ecuador was funded by Secretaría Nacional de Educación Superior, Ciencia, Tecnología e Innovación del Ecuador SENESCYT (Arca de Noé initiative; SRR and Omar Torres principal investigators) and grants from Pontificia Universidad Católica del Ecuador, Dirección General Académica. We are grateful to the staff of the Servicio Nacional de Áreas Naturales Protegidas por el Estado (SERNANP), especially the rangers and volunteers, for their cooperation and for the required research permits. We also thank L. Ríos of Consultores Asociados en Naturaleza y Desarrollo (CANDES) and W.

Nañez of CORBIDI for the logistic support in the field, and D. Matos and A. Orihuela from Ministerio del Ambiente (MINAM) for the coordination with the SERNANP. The field work was funded by the MINAM.

References

Altig R, Johnston GF (1989) Guilds of anuran larvae: relationships among developmental modes, morphologies, and habitats. Herpetological monographs: 81–109. https://doi.org/10.2307/1466987

Altig R, McDiarmid RW (1999) Body plan: development and morphology. In: McDiarmid RW, Altig R (Eds) Tadpoles, the Biology of Anuran Larvae. The University of Chicago Press, Chicago and London, 24–51.

Blotto BL, Lyra ML, Cardoso MCS, Trefaut Rodrigues M, Dias IR, Marciano-Jr E, Dal Vechio F, Orrico VGD, Brandão RA, Lopes de Assis C (2021) The phylogeny of the casque-headed treefrogs (Hylidae: Hylinae: Lophyohylini). Cladistics 37: 36–72. https://doi.org/10.1111/cla.12409

Brack-Egg E (1986) Las ecorregiones del Perú. Boletín de Lima 44: 57–70.

Caminer MA, Ron SR (2014) Systematics of treefrogs of the *Hypsiboas calcaratus* and *Hypsiboas fasciatus* species complex (Anura, Hylidae) with the description of four new species. Zookeys 370: 1–68. https://doi.org/10.3897/zookeys.370.6291

Chasiluisa VD, Caminer MA, Varela-Jaramillo A, Ron SR (2020) Description and phylogenetic relationships of a new species of treefrog of the *Osteocephalus buckleyi* species group (Anura: Hylidae). Neotropical Biodiversity 6: 21–36. https://doi.org/10.1080/23766808.2020.1729306

Coloma LA, Carvajal-Endara S, Duenas JF, Paredes-Recalde A, Morales-Mite M, Almeida-Reinoso D, Tapia EE, Hutter CR, Toral E, Guayasamin JM (2012) Molecular phylogenetics of stream treefrogs of the Hyloscirtus larinopygion group (Anura: Hylidae), and description of two new species from Ecuador. Zootaxa 3364: 1–78. https://doi.org/10.11646/zootaxa.3364.1.1

de Queiroz K (1998) The general lineage concept of species, species criteria, and the process of speciation. In: Howard DJ, Berlocher SH (Eds) Endless Forms: Species and Speciation. Oxford University Press, UK, 57–75.

de Queiroz K (2007) Species concepts and species delimitation. Systematic Biology 56: 879–886. https://doi.org/10.1080/10635150701701083

Duellman WE (1970) Hylid frogs of Middle America (Vol. 1). Museum of Natural History University of Kansas, USA, 753 pp. https://doi.org/10.5962/bhl.title.2835

Duellman WE (2019) The last one: a new species of *Osteocephalus* (Anura: Hylidae) from Colombia, with comments on the morphological and behavioral diversity within the genus. Phyllomedusa: Journal of Herpetology 18: 141–157. https://doi.org/10.11606/issn.2316-9079.v18i2p141-157

Ferrão M, Moravec J, Moraes LJCL, de Carvalho VT, Gordo M, Lima AP (2019) Rediscovery of *Osteocephalus vilarsi* (Anura: Hylidae): an overlooked but widespread Amazonian spiny-backed treefrog. PeerJ 7: e8160. https://doi.org/10.7717/peerj.8160

Frost DR (2023) Amphibian Species of the World: an Online Reference. Version 6.1. https://amphibiansoftheworld.amnh.org/index.php [accessed 10 January 2023.2023]

Goebel AM, Donnelly JM, Atz ME (1999) PCR primers and amplification methods for 12S ribosomal DNA, the control region, cytochrome oxidase I, and cytochromebin bufonids and other frogs, and an overview of PCR primers which have amplified DNA in amphibians successfully. Molecular Phylogenetics and Evolution 11: 163–199. https://doi.org/10.1006/mpev.1998.0538

Gosner KL (1960) A simplified table for staging anuran embryos and larvae with notes on identification. Herpetologica 16: 183–190. https://doi.org/10.1093/sysbio/syq010

Guindon S, Dufayard J-F, Lefort V, Anisimova M, Hordijk W, Gascuel O (2010) New algorithms and methods to estimate maximum-likelihood phylogenies: assessing the performance of PhyML 3.0. Systematic Biology 59: 307–321. https://doi.org/10.1093/sysbio/syq010

Henle K (1981) *Argenteohyla altamazonica*, ein neuer Hylide mit paarigen, lateralen Schallblasen aus Peru (Amphibia: Salientia: Hylidae). Amphibia-Reptilia 2: 133–137. https://doi.org/10.1163/156853881X00177

Hero J-M (1990) An illustrated key to tadpoles occurring in the Central Amazon rainforest, Manaus, Amazonas, Brasil. Amazoniana: Limnologia et Oecologia Regionalis Systematis Fluminis Amazonas 11: 201–262.

Hoang DT, Chernomor O, von Haeseler A, Minh BQ, Vinh LS (2018) UFBoot2: Improving the Ultrafast Bootstrap Approximation. Molecular Biology and Evolution 35: 518–522. https://doi.org/10.1093/molbev/msx281

Jungfer K-H (2010) The taxonomic status of some spiny-backed treefrogs, genus *Osteocephalus* (Amphibia: Anura: Hylidae). Zootaxa 2407: 28–50. https://doi.org/10.11646/zootaxa.2407.1.2

Jungfer K-H (2011) A new tree frog of the genus *Osteocephalus* from high altitudes in the Cordillera del Cóndor, Ecuador (Amphibia: Anura: Hylidae). The Herpetological Journal 21: 247–253.

Jungfer K-H, Faivovich J, Padial JM, Castroviejo-Fisher S, Lyra MM, Berneck BVM, Iglesias PP, Kok PJR, MacCulloch RD, Rodrigues MT, Verdade VK, Torres Gastello CP, Chaparro JC, Valdujo PH, Reichle S, Moravec J, Gvoždík V, Gagliardi-Urrutia G, Ernst R, De la Riva I, Means DB, Lima AP, Señaris JC, Wheeler WC, Haddad CFB (2013) Systematics of spiny-backed treefrogs (Hylidae: *Osteocephalus*): an Amazonian puzzle. Zoologica Scripta 42: 351–380. https://doi.org/10.1111/zsc.12015

Jungfer K-H, Hödl W (2002) A new species of *Osteocephalus* from Ecuador and a redescription of *O. leprieurii* (Duméril & Bibron, 1841)(Anura: Hylidae). Amphibia-Reptilia 23: 21–46. https://doi.org/10.1163/156853802320877609

Jungfer K-H, Ron S, Seipp R, Almendáriz A (2000) Two new species of hylid frogs, genus *Osteocephalus*, from Amazonian Ecuador. Amphibia-Reptilia 21: 327–340. https://doi.org/10.1163/156853800507525

Jungfer K-H, Verdade VK, Faivovich J, Rodrigues MT (2016) A new species of spiny-backed treefrog (*Osteocephalus*) from Central Amazonian Brazil (Amphibia: Anura: Hylidae). Zootaxa 4114: 171–181. https://doi.org/10.11646/zootaxa.4114.2.6

Jungfer K-H, Weygoldt P (1999) Biparental care in the tadpole-feeding Amazonian treefrog *Osteocephalus oophagus*. Amphibia-Reptilia 20: 235–249. https://doi.org/10.1163/156853899X00277

Jungfer KH, Schiesari LC (1995) Description of a central Amazonian and Guianan tree frog, genus *Osteocephalus* (Anura, Hylidae), with oophagous tadpoles. Alytes 13: 1–13.

Katoh K, Standley DM (2013) MAFFT multiple sequence alignment software version 7: improvements in performance and usability. Molecular biology and evolution 30: 772–780. https://doi.org/10.1093/molbev/mst010

Kearse M, Moir R, Wilson A, Stones-Havas S, Cheung M, Sturrock S, Buxton S, Cooper A, Markowitz S, Duran C (2012) Geneious Basic: an integrated and extendable desktop software platform for the organization and analysis of sequence data. Bioinformatics 28: 1647–1649. https://doi.org/10.1093/bioinformatics/bts199

Lehr E, Faivovich J, Jungfer KH (2011) Description of the tadpoles of *Hypsiboas aguilari* and *H. melanopleura* (Anura: Hylidae: Hypsiboas pulchellus group).

Lima AP, Magnusson WE, Menin M, Erdtmann LK, Rodrigues DdJ, Keller C, Hödl W (2012) Guia de sapos da Reserva Adolpho Ducke-Amazônia Central.

Lynch JD, Duellman WE (1997) Frogs of the genus *Eleutherodactylus* (Leptodactylidae) in western Ecuador: Systematic, Ecology, and Biogeography. Natural History Museum, The University of Kansas, Lawrence, 236 pp. https://doi.org/10.5962/bhl.title.7951

Maddison WP, Maddison DR (2019) Mesquite: a modular system for evolutionary analysis. version 3.61 pp.

Melo-Sampaio PR, Ferrão M, de Lima Moraes LJC (2021) A new species of *Osteocephalus* Steindachner, 1862 (Anura, Hylidae), from Brazilian Amazonia. Breviora 572: 1–21. https://doi.org/10.3099/0006-9698-572.1.1

Menin M, da Silva Melo L, Lima AP (2011) The tadpole of *Osteocephalus cabrerai* (Anura: Hylidae) from central Amazonia, Brazil. Phyllomedusa: Journal of Herpetology 10: 137–142. https://doi.org/10.11606/issn.2316-9079.v10i2p137-142

Minh BQ, Schmidt HA, Chernomor O, Schrempf D, Woodhams MD, Von Haeseler A, Lanfear R (2020) IQ-TREE 2: new models and efficient methods for phylogenetic inference in the genomic era. Molecular biology and evolution 37: 1530–1534. https://doi.org/10.1093/molbev/msaa015

Moen DS, Wiens JJ (2009) Phylogenetic evidence for competitively driven divergence: body-size evolution in Caribbean treefrogs (Hylidae: *Osteopilus*). Evolution: International Journal of Organic Evolution 63: 195–214. https://doi.org/10.1111/j.1558-5646.2008.00538.x

Moravec J, Aparicio J, Guerrero-Reinhard M, Calderon G, Jungfer K-H, Gvoždík V (2009) A new species of *Osteocephalus* (Anura: Hylidae) from Amazonian Bolivia: first evidence of tree frog breeding in fruit capsules of the Brazil nut tree. Zootaxa 2215: 37–54.

Myers CW, Duellman WE (1982) A new species of *Hyla* from Cerro Colorado, and other tree frog records and geographical notes from western Panama. American Museum of Natural History, New York.

Nguyen L-T, Schmidt HA, von Haeseler A, Minh BQ (2015) IQ-TREE: A fast and effective stochastic algorithm for estimating maximum-likelihood phylogenies. Molecular biology and evolution 32: 268–274. https://doi.org/10.1093/molbev/msu300

Ortiz DA, Hoskin CJ, Werneck FP, Réjaud A, Manzi S, Ron SR, Fouquet A (2022) Historical biogeography highlights the role of Miocene landscape changes on the diversification of a clade of Amazonian tree frogs. Organisms Diversity & Evolution: 1–20. https://doi.org/10.1007/s13127-022-00588-2

Peñaherrera del Aguila C (1989) Atlas del Perú. Instituto Geográfico Nacional, Lima, 400 pp.

Ron SR, Toral E, Venegas PJ, Barnes CW (2010) Taxonomic revision and phylogenetic position of *Osteocephalus festae* (Anura, Hylidae) with description of its larva. ZooKeys 70: 67–92. https://doi.org/10.3897/zookeys.70.765

Ron SR, Venegas PJ, Toral E, Morley R, Diego AO, Manzano AL (2012) Systematics of the *Osteocephalus buckleyi* species complex (Anura, Hylidae) from Ecuador and Peru. Zookeys 229: 1–52. https://doi.org/10.3897/zookeys.229.3580

Sambrook J, Fritsh EF, Maniatis T (1989) Molecular Colning: a Laboratory Manual. Cold Spring Harbour Lab. Press, New York, 1626 pp.

Schiesari LC, Grillitsch B, Vogl C (1996) Comparative morphology of phytotelmonous and pond-dwelling larvae of four neotropical treefrog species (Anura, Hylidae, *Osteocephalus oophagus*, *Osteocephalus taurinus*, *Phrynohyas resinifictrix*, *Phrynohyas venulosa*). Alytes 13: 109–139.

Tamura K, Stecher G, Kumar S (2021) MEGA11: molecular evolutionary genetics analysis version 11. Molecular biology and evolution 38: 3022–3027. https://doi.org/10.1093/molbev/msab120

To T-H, Jung M, Lycett S, Gascuel O (2016) Fast dating using least-squares criteria and algorithms. Systematic Biology 65: 82–97. https://doi.org/10.1093/sysbio/syv068

Trueb L, Duellman WE (1970) The systematic status and life history of *Hyla verrucigera* Werner. Copeia: 601–610. https://doi.org/10.2307/1442303

Trueb L, Duellman WE (1971) Synopsis of neotropical Hylid frogs, genus *Osteocephalus*. Occasional Papers of the Museum of Natural History, University of Kansas, Kansas, 47 pp.

Venkatesh B, Erdmann MV, Brenner S (2001) Molecular synapomorphies resolve evolutionary relationships of extant jawed vertebrates. Proceedings of the National Academy of Sciences 98: 11382–11387. https://doi.org/10.1073/pnas.201415598

Villacampa Ortega J, Whitworth A, Burdekin O (2013) *Osteocephalus mimeticus* (Melin, 1941)(Amphibia: Anura: Hylidae): New locality, range extension and notes on distribution. Check List 9: 1126–1128. https://doi.org/10.15560/9.5.1126

Wiens JJ, Fetzner Jr JW, Parkinson CL, Reeder TW (2005) Hylid frog phylogeny and sampling strategies for speciose clades. Systematic Biology 54: 778–807. https://doi.org/10.1080/10635150500234625

Supplementary material 1

Additional specimens examined

Author: Pablo J. Venegas

Data type: Metadata of examined specimens

Explanation note: Metadata of examined specimens, including collection locality and catalog number.

Copyright notice: This dataset is made available under the Open Database License (http://opendatacommons.org/licenses/odbl/1.0). The Open Database License (ODbL) is a license agreement intended to allow users to freely share, modify, and use this Dataset while maintaining this same freedom for others, provided that the original source and author(s) are credited.

Link: https://doi.org/10.3897/evolsyst.7.102360.suppl1